Acta Chemica Scandinavica B 31 (1977) 171—181

An X-Ray Investigation of Some Aqueous Zirconium(IV) Halide, a Hafnium(IV) Chloride, and Some Zirconium(IV) Perchlorate Solutions

MÄRTHA ÅBERG

Department of Inorganic Chemistry, Royal Institute of Technology, S-100 44 Stockholm 70, Sweden

The X-ray scattering from aqueous zirconium(IV) halide, hafnium(IV) chloride, and zirconium(IV) perchlorate solutions has been measured. The mol ratios X/Zr = 1 and 2 (X = Cl or Br) and Cl/Hf = 2 have been studied. The mol ratio ClO_4/Zr has been varied from 1.7 to 4.3. The experimental data, excluding X/Zr = 1, are consistent with the formation of a predominant tetranuclear complex, $[M_4(OH)_8(H_2O)_{16}]^{8+}$ (M = Zr or Hf), with a structure similar to that of $[Zr_4(OH)_8(H_2O)_{16}]Cl_8 \cdot 12H_2O$ ($= ZrOCl_2 \cdot 8H_2O$) known from the solid state. Part of the halide ions are associated with the complex, and possible sites for these ions are discussed. For X/Zr = 1 the scattering data indicate the formation of polymers, $[Zr_4O_x(OH)_{12-x}(H_2O)_{8+2x}]_n^{4+}$, built up from the discrete tetramers, $(Zr_4(OH)_8(H_2O)_{16}]^{8+}$, linked to each other through new O or double HO bridges in a random way.

Zr(IV) and Hf(IV) are known to undergo complicated hydrolysis even in very acidic aqueous solutions. The large amount of experimental results from solution chemistry studies of these metal ions has been reviewed by, *e.g.*, Solovkin and Tsvetkova,[1] Caletka,[2] Hala,[3] and Larsen.[4] From a compilation of published data Solovkin and Tsvetkova have concluded that there is no justification for the existence of the zirconyl ion, ZrO^{2+}, in aqueous solutions. The infrared [5] and Raman [6] spectra of some Zr(IV) salts also show no evidence for the presence of the Zr = O group.

The predominant hydrolyzed complexes of Zr(IV) and Hf(IV) are polynuclear even in very dilute ($> 10^{-4} - 10^{-3}$ M) solutions of high acidity (1 – 2 M). Various experimental techniques such as ultracentrifugation, spectrophotometry, potentiometry, light scattering, diffusion, and extraction have been utilized to characterize these complexes.[7] Species such as $M_3(OH)_4^{8+}$ and $M_4(OH)_8^{8+}$ have been suggested, and in some investigations formation constants have been derived from the experimental data. The studies are complicated by the slowness with which the systems attain equilibrium.

Direct proofs for the existence of discrete polymeric species have been provided by Clearfield and Vaughan [8] and by Mak [9] through the determination of the crystal structure of $ZrOCl_2 \cdot 8H_2O$. This structure, which will be discussed more in detail below, is built up from the tetramers $[Zr_4(OH)_8(H_2O)_{16}]^{8+}$ linked to each other through chloride ions and water molecules. An X-ray diffraction study of aqueous solutions of zirconium and hafnium halides has been carried out by Muha [10] to see whether or not the tetramer $[M_4(OH)_8(H_2O_{16}]^{8+}$ remains intact when the compound $MOX_2 \cdot 8H_2O$ is dissolved. The results, which will also be discussed below, indicate that a tetramer with a structure similar to that in the solid state is the predominant complex in solution.

Thus, it has now been clearly shown that tetramers are the predominant polynuclear complexes for Y/M = 2, where Y is a weak complexing anion like Cl^-, Br^-, or ClO_4^-. But very little is known about the structures of the species at other stages during the hydrolysis. In the present investigation zirconium perchlorate solutions with ClO_4/Zr mol ratios between 1.7 and 4.3 have been studied to see what structural

changes occur on acidification. No solutions with $X/Zr > 2.5$ (X = Cl or Br) and a sufficiently high total concentration of Zr can be prepared because the solubility of $ZrOX_2 \cdot 8H_2O$ decreases as the amount of excess acid is increased. Also two zirconium halide solutions with $X/Zr = 1$, the minimum value obtainable, have been studied. Here higher complexes than tetramers are suggested to be the predominating species.[4] As the data collected by Muha[10] are not as accurate as those which can now be obtained, the scattering from some solutions with $X/M = 2$ has also been measured for comparison.

EXPERIMENTAL

Preparation and analysis of the solutions. Hydrous ZrO_2 (zirconium hydroxide) was precipitated by NH_3 from aqueous solutions of $ZrOCl_2 \cdot 8H_2O$ (*p.a.*). It was then dissolved in aqueous HCl, HBr, or $HClO_4$ of known concentrations. HfO_2 (*p.a.*) was melted with $Na_2B_4O_7 \cdot 10H_2O$ and the melt was then dissolved in HCl. Hydrous HfO_2 (hafnium hydroxide) was precipitated from the solution by NH_3 and was subsequently dissolved in aqueous HCl of known concentration. All solutions were allowed to stand on the water bath for about one month before measurements were performed.

The amount of Zr or Hf was determined by precipitation using NH_3 and ignition of the hydroxide to ZrO_2 or HfO_2. The total amount of anion present was determined by passing a portion of the solution, from which the metal ions had been removed by precipitation and filtration, through an H^+-saturated cation exchanger. The free acid was then titrated with standardized NaOH. The densities of the solutions were determined pycnometrically.

The compositions of the solutions investigated are given in Table 1.

Measurements of the X-ray scattering. The diffractometer was the same as described previously.[11–13] Mo*K* radiation ($\lambda_{K\alpha} = 0.7107$ Å) was used for the measurements on the hafnium solution. For the zirconium solutions all scattering curves were measured with Ag*K* radiation ($\lambda_{K\alpha} = 0.5608$ Å) to avoid fluorescence. A Philips X-ray generator PW 1130 was used. All measurements were carried out at 25 °C.

The scattering was measured at discrete points from $\theta = 1°$ up to $\theta = 70°$, 2θ being the scattering angle. The opening slits used were 1/12, 1/4, and 1°. The scattering data were recalculated to a common slit width from measurements in overlapping regions. Usually 40 000 counts were taken for each point corresponding to a statistical error of 0.5 %. For $\theta < \sim 20°$ (or 6° for some solutions) points were measured at intervals of 0.1° and for $\theta > \sim 20°$ (or 6°) intervals of 0.25° were used. All measurements were made twice.

Treatment of the intensity data. All calculations were carried out on an IBM 360/75 computer with the use of the KURVLR and PUTSLR programs.[14]

The measured intensity data were corrected for polarization in the sample and in the mono-

Table 1. Compositions of the solutions. The volume of a stoichiometric unit of solution containing one Zr(Hf) atom = V (Å^3). n_{HO} = number of HO groups per Zr(Hf) atom as estimated from the analyses. I = halide solutions, II = perchlorate solutions.

Solution	I:1	I:2	I:3	I:4	I:5	II:1	II:2	II:3	II:4	II:5
Concentration in mol/l										
Hf	1.729									
Zr		2.598	3.822	3.124	3.269	2.663	2.880	3.007	2.445	2.074
Br				6.418	3.235					
Cl	3.485	4.974	4.003			4.462	6.689	8.409	8.649	8.925
O	55.52	55.18	57.58	51.98	56.02	67.00	70.94	73.05	72.96	72.59
H	107.61	104.95	103.87	97.89	102.21	92.12	83.53	75.21	75.59	74.41
Number of atoms in the unit of volume V										
Hf	1.000									
Zr		1.000	1.000	1.000	1.000	1.000	1.000	1.000	1.000	1.000
Br				2.055	0.990					
Cl	2.015	1.914	1.047			1.675	2.322	2.797	3.537	4.303
O	32.10	21.24	15.06	16.64	17.14	25.16	24.63	24.30	29.84	35.00
H	62.22	40.39	27.17	31.34	31.27	34.59	29.00	25.01	30.92	35.88
n_{HO}	1.985	2.086	2.953	1.945	3.010	2.325	1.678	1.203	0.463	−0.303
V	960.2	639.0	434.4	531.6	508.0	623.5	576.6	552.3	679.2	800.6

chromator by dividing by the factor $(1+\cos 2\alpha \cos^2 2\theta)/(1+\cos 2\alpha)$, where 2α is the scattering angle at the monochromator.[14] Corrections for multiple scattering were applied, but they were almost negligible.[14] The incoherent scattering passing through the monochromator was estimated in the way described previously.[11,13,15]

For each solution the intensities were normalized to a stoichiometric unit of volume containing one Zr or Hf atom (Table 1). The scaling was done by comparing the observed intensities corrected for polarization and multiple scattering, $I_{corr}(s)$, where $s=4\pi \sin\theta/\lambda$, with the calculated sum of the independent coherent and the incoherent scattering in the high-angle region ($\theta > 55°$).

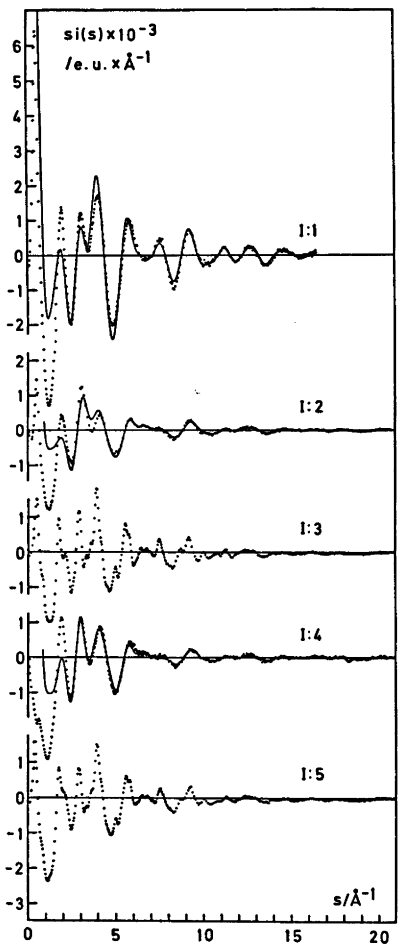

Fig. 1a. Reduced intensity functions, $i(s)$, multiplied by s for the halide solutions. The experimental values are given as dots. The full-drawn curves represent intramolecular contributions calculated with the use of parameters given by Mak,[9] in Table 2, and in the text.

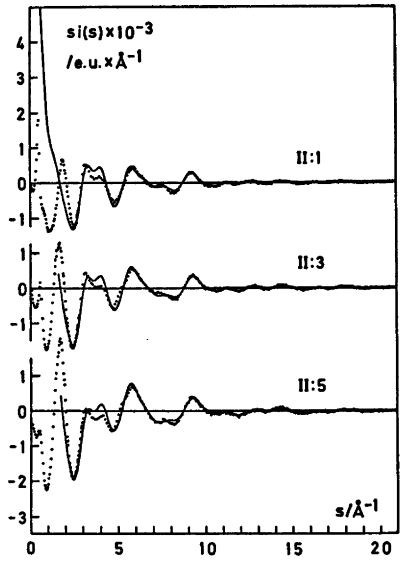

Fig. 1b. $si(s)$ functions for three of the perchlorate solutions. The fulldrawn curves have been calculated with the use of parameters given by Mak [9] and in the text.

The reduced intensity data, $i(s)$, were corrected for low-frequency additions resulting in spurious peaks below 1 Å in the radial distribution curves, which could not correspond to interatomic distances.[14]

From the reduced intensity values the electronic radial distribution functions were calculated:

$$D(r) = 4\pi r^2 \varrho_0 + 2r/\pi \int_0^{s_{max}} si(s)M(s) \sin(rs)ds \quad (1)$$

The modification function, $M(s)$, was chosen to be $[f_{Zr}^2(0)/f_{Zr}^2(s)]\exp(-0.01s^2)$ and corresponding for Hf. ϱ_0 is the average scattering density given by the square of the number of electrons per unit volume (V in Table 1). The observed $i(s)$ values were used for the integration, *i.e.*, no attempt was made to draw a smooth curve through the experimental points.

Theoretical pair interaction functions were calculated from:

$$i_{pq}(s) = \sum_p \sum_{q \neq p} [f_p(s)f_q(s) + \Delta f_p'' \Delta f_q''] \sin(r_{pq}s) \times (r_{pq}s)^{-1} \exp(-b_{pq}s^2) \quad (2)$$

Here r_{pq} is the distance between the atoms p and q and b_{pq} is a temperature factor related to the root mean square variation u_{pq} of the distance r_{pq} by $b_{pq}=u_{pq}^2/2$.

The Fourier inversion of $\sum i_{pq}(s)$ was made in the same way as that of the experimental reduced intensities.

The scattering factors, $f(s)$, used were those given by Cromer and Waber [16] for Hf, Zr, Br, Cl, and O. For H the values given by Stewart *et al.*[17] were used. Corrections for anomalous dispersion, $\Delta f'$ and $\Delta f''$, were taken from Cromer.[18] Values for the incoherent radiation were taken from Cromer [19] for Hf, Zr, Br, Cl, and O and from Compton and Allison [20] for H. They were corrected for the Breit-Dirac factor.

Tables of the normalized intensities and of the reduced intensity values for the investigated solutions are available from the author on request. The normalized intensities are corrected for incoherent radiation and the reduced intensity values corrected for spurious peaks below 1 Å. The reduced intensity values in the form $si(s)$ are also shown in Figs. 1a and 1b.

ANALYSIS OF THE DATA

Radial distribution curves, $D(r)$, are given in Figs. 2a and 2b, and $D(r)-4\pi r^2\varrho_0$ functions are shown in Figs. 3a and 3b.

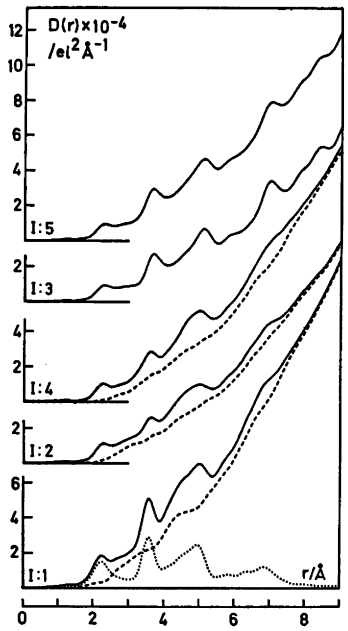

Fig. 2a. Radial distribution curves, $D(r)$, for the halide solutions. The dashed curves are the differences between the experimental functions and the calculated intramolecular contributions. The sum of the intramolecular contributions is also given separately for solution I:1.

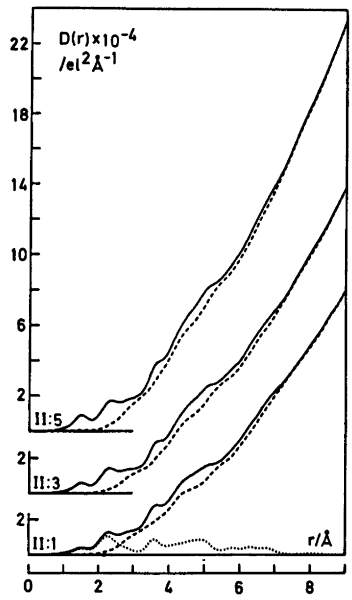

Fig. 2b. $D(r)$ curves for three of the perchlorate solutions. The sum of the intramolecular contributions is given separately for solution II:1.

Early X-ray scattering data on aqueous solutions of $MOX_2 \cdot 8H_2O$ (M = Zr or Hf, X = Cl or Br) collected by Muha [10] were explained by assuming the existence of a complex $[M_4(OH)_8(H_2O)_{16}]X_8$ with a structure similar to that which at that time was known from the solid state. But in the first crystal structure determination of $ZrOCl_2 \cdot 8H_2O$ made by Clearfield and Vaughan [8] from two-dimensional data, only the Zr atoms were located with any degree of accuracy. Later on, a refinement of the structure based on three-dimensional data was carried out by Mak.[9] He found the main features of the old structure to be correct, but the coordination polyhedron of O atoms about each Zr atom to be more closely related to the dodecahedron rather than the square antiprism suggested by Clearfield and Vaughan. The structure is built up from discrete $[Zr_4(OH)_8(H_2O)_{16}]^{8+}$ tetramers linked to each other through a network of Cl^- ions and water molecules. In the tetramer (Fig. 4) the Zr atoms are in a slightly puckered square configuration. Adjacent Zr atoms are joined through double HO bridges with one O atom above and the other below the mean square plane. The dis-

torted dodecahedron about each Zr atom is completed by terminal O atoms from four coordinated water molecules.

With the use of the positional parameters from the crystal structure determined by Mak the expected peak shapes for the tetramer $Zr_4O_8O_{16}$ (H atoms being omitted) were calculated. The temperature factors were assumed to be 0.003 Å² for Zr – Zr interactions, 0.0065 Å² for Zr – O interactions, and 0.01 Å² for O – O interactions. The calculated peak shapes are shown in Fig. 5. Comparison with the functions $D(r) - 4\pi r^2\varrho_0$ in Figs. 3a and 3b and also with the $D(r)$ functions in Figs. 2a and 2b shows similar peaks to be present for all the solutions investigated, halide as well as perchlorate solutions, except the zirconium halide solutions with $n_{HO} = 3$. These two solutions behave differently and will be discussed separately.

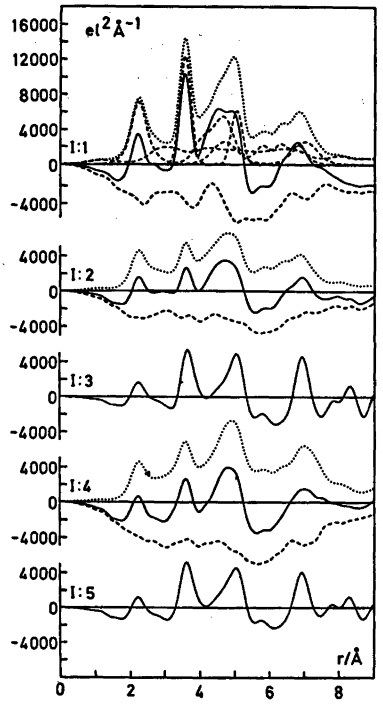

Fig. 3a. Functions $D(r) - 4\pi r^2\varrho_0$ (full-drawn) for the halide solutions and theoretical peak shapes for the $M_4O_8O_{16}X_8$ complex (dotted). The lower dashed curves are obtained when the calculated peak shapes are subtracted from the experimental $D(r) - 4\pi r^2\varrho_0$ curves. For solution I:1 the Hf – Hf, Hf – O, Hf – Cl, and light-atom interactions are drawn separately (upper dashed curves).

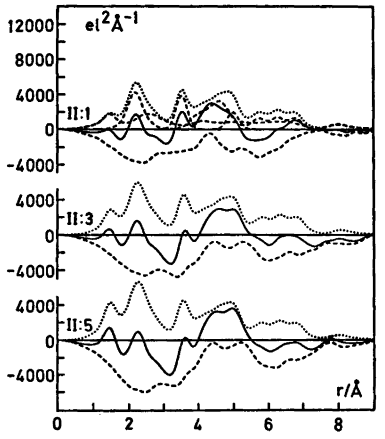

Fig. 3b. Functions $D(r) - 4\pi r^2\varrho_0$ for three of the perchlorate solutions and theoretical peak shapes for the $Zr_4O_8O_{16}$ and ClO_4^- complexes. For solution II:1 the Zr – Zr, Zr – O, and light-atom interactions are drawn separately (upper dashed curves).

Fig. 5 also shows the difference curve obtained when the sum of the intramolecular interactions within the $Zr_4O_8O_{16}$ group is subtracted from the experimental $D(r) - 4\pi r^2\varrho_0$ function for solution I:2. This curve represents the remaining interactions in the solutions. Broad peaks are found around 3.1, 4.6, and 7.0 Å. They contain contributions from the coordination of the Cl^- ions and from that part of the water structure which has not been broken down by the solute species. All intermolecular interactions will also contribute to the remaining structure of the solution.

The halide solutions with $n_{HO} = 2$

Analyses of the intramolecular interactions within the $M_4O_8O_{16}$ group (M = Zr or Hf) for the three halide solutions with $n_{HO} = 2$ were made by least squares refinement procedures using the PUTSLR program.[14] The experimental reduced intensity values, $i(s)$, were compared with $\sum i_{pq}(s)$ values calculated from eqn. (2). For each pair interaction a distance r_{pq}, a temperature factor b_{pq}, and a frequency factor n_{pq} were introduced as parameters that could be varied. A minimum was sought for the error square sum $U = \sum w(s)[i(s) - \sum i_{pq}(s)]^2$. The weighting function $w(s) = \cos\theta / I_{corr}^2(s)$ was chosen. With

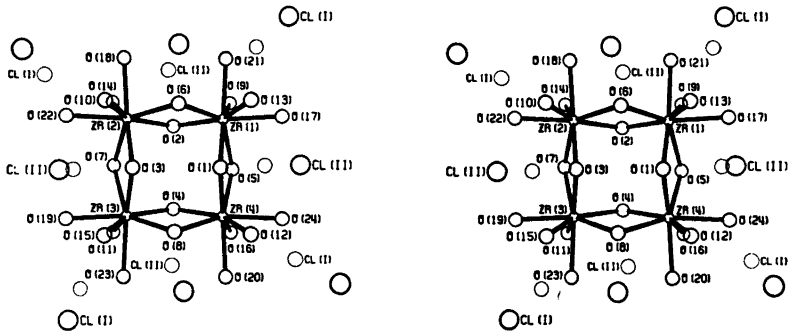

Fig. 4. A stereoscopic view of the tetranuclear complex $[Zr_4(OH)_8(H_2O)_{16}]^{8+}$ drawn with the use of the positional parameters given by Mak.[9] The two chloride sites, Cl(I) and Cl(II), outside the complex are also shown.

this weighting function the contribution to U from each experimental point is inversely proportional to the square of its estimated standard deviation.

As the curves in Fig. 5 indicate that no significant deviations from the positional parameter values obtained by Mak [9] seem to occur for $Zr_4O_8O_{16}$ in solution I:2, only the temperature factors for the interactions within the $M_4O_8O_{16}$ complex were adjusted by means of the least squares procedures. Experimental data for $s_{min} < s < s_{max}$, where $s_{max} = 16$ Å^{-1} (MoK radiation) or 20 Å^{-1} (AgK radiation), were used, s_{min} being varied from 6.5 to 10 Å^{-1}. The average values obtained were: $b_{M-M} = 0.0030(1)$ Å^2, $b_{M-O} = 0.0035(2)$ Å^2, and $b_{O-O} = 0.0040(3)$ Å^2.

With the use of the refined values of the temperature factors theoretical curves similar to those in Fig. 5 were calculated for the three halide solutions with $n_{HO} = 2$. The new difference curves are shown in Fig. 6. Because of the high charge of the $[M_4(OH)_8(H_2O)_{16}]^{8+}$ complex it seems reasonable to assume that halide ions are arranged in a second coordination sphere outside the tetramer, probably being held in place by electrostatic forces. In the solid state many Zr–Cl distances are found in the regions 4.6–5.0 and 7.0–7.3 Å.[9] The residual peaks at these r values have thus been assigned to M–X interactions. Further support for such an interpretation is given by the sizes of the peaks which correspond to about two M–X interactions/M atom in each of the two regions. In addition the difference curves in Fig. 6 indicate that for the zirconium bromide solu-

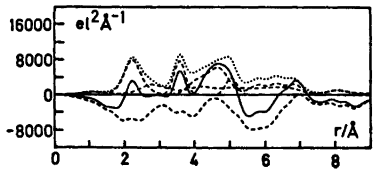

Fig. 5. Expected peak shapes for the tetramer $Zr_4O_8O_{16}$ calculated from the positional parameters given by Mak.[9] The upper dashed curves represent Zr–Zr, Zr–O, and O–O interactions. The dotted curve gives the sum of all intramolecular interactions. The lower dashed curve is the difference between the $D(r) - 4\pi r^2\varrho_0$ for solution I:2 (full-drawn curve) and the sum of the intramolecular interactions within the tetramer.

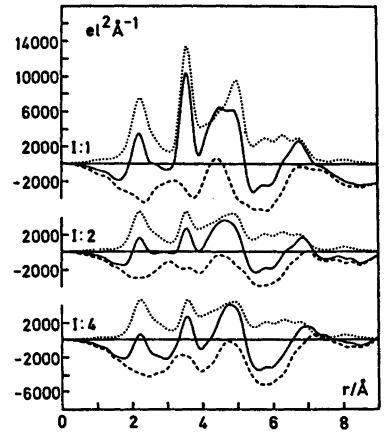

Fig. 6. Difference curves for the halide solutions with $n_{HO} = 2$ (dashed) obtained by subtracting the calculated peak shapes for the $M_4O_8O_{16}$ complex (dotted) from the experimental $D(r) - 4\pi r^2\varrho_0$ functions (full-drawn).

Table 2. Parameters for the halide ions. (X,Y,Z) are the positional parameters (Å) in a coordinate system with the origin at the centre of the M_4 square and the x and y axes directed horizontally and vertically, respectively, (Fig. 4), r_{M-X} = M − X distance (Å), b = temperature factor (Å²), and n_{M-X} = frequency factor (number of M − X distances/M atom).

Solution	(X,Y,Z) [a]	r_{M-X}	b_{X-X} b_{M-O}
I:1	3.79, 0, ± 3.83	4.68 6.99	0.043 [c]
I:2	3.79, 0, ± 3.83	4.68 6.99	0.043 [c]
I:4	3.89(2),0, ± 3.96(2) [b]	4.83 7.14	0.043(2) [bc]

[a] Remaining parameter values are obtained from the S_4 point group symmetry. [b] These values were obtained from a least squares refinement series using experimental data for 2.2 Å^{-1} < s < 8.8 Å^{-1}. [c] $n_{M-X}(=\frac{1}{2}n_{M-X}^{max})=2$. Non-coordinated halide ions are assumed to be octahedrally surrounded by water molecules ($r_{Cl-O}=3.1$ Å, $r_{Br-O}=3.25$ Å, $b_{X-O}=0.043$ Å²) when parameters from this table are used for calculations of theoretical peak shapes.

tion the M − X distances are longer than those for the two chloride solutions.

Preliminary theoretical peak shapes based on the rather irregular arrangement of halide ions in the positions II in the solid state (Fig. 4), four M − X distances per M atom in each of the two regions, gave a rather good explanation of the experimental data when an occupancy factor of 0.5 was used. Therefore, the halide positions II were arranged more symmetrically, and a least squares refinement series was performed using data for the zirconium bromide solution. Three parameters were varied: two positional parameters and one temperature factor. The results are given in Table 2.

Theoretical peak shapes for the complexes $M_4O_8O_{16}X_8$ with the parameters for the halide ions taken from Table 2 are shown in Fig. 3a. They seem to give a satisfactory explanation of the experimental data for the zirconium halide solutions with $n_{HO}=2$ (I:2 and I:4). But for the hafnium chloride solution (I:1) there is a residual peak at 4.3 Å which is too pronounced to be due only to the highly damped intermolecular interactions. As this peak may be interpreted in many different ways, no additional structural models including interactions at 4.3 Å have been tested quantitatively.

For the positions I in the solid state (Fig. 4) the Zr − Cl distances range from 4.9 to 10.2 Å. Due to this spread no pronounced difference is obtained when these positions are included in the structural model for the solutions. For a more symmetrical arrangement of the positions I, there are for each Zr atom: two Zr − Cl distances at about 4.7 Å, four at about 7.0 Å, and two at about 8.7 Å which do not seem to be in very good agreement with the difference curves in Fig. 6. This means that the positions I alone do not give a satisfactory explanation of the experimental data and that no better agreement is obtained on adding these positions to a structural model including the positions II.

The perchlorate solutions

Because of the low atomic number of Zr the ClO_4 groups contribute relatively more to the X-ray scattering in the zirconium perchlorate solutions than in, *e.g.*, the mercury perchlorate solutions investigated previously.[13] For this reason, the distance and the temperature factor for the Cl − O interaction in a tetrahedral ClO_4 group were refined in a series of least squares procedures. The temperature factor for the O − O interactions was kept constant at 0.004 Å². Theoretical intensity values for the $Zr_4O_8O_{16}$ complex calculated with the same parameters, as were used for Fig. 6, were introduced as a constant background during the refinements. Experimental data for $s_{min} < s < 20$ Å^{-1} were used, and s_{min} was varied from 4 to 10 Å^{-1}. The average values obtained were: $r_{Cl-O}=1.465(4)$ Å ($r_{O-O}=2.40$ Å) and $b_{Cl-O}=0.0031(3)$ Å².

In a second step of the least squares refinements the temperature factors for the interactions within the $Zr_4O_8O_{16}$ complex were adjusted. Experimental data for $s_{min} < s < 20$ Å^{-1} with s_{min} varying from 4 to 10 Å^{-1} were used. The average values obtained were: $b_{Zr-Zr}=0.0028(1)$ Å², $b_{Zr-O}=0.0037(3)$ Å², and $b_{O-O}=0.0046(5)$ Å². Calculated peak shapes for the $Zr_4O_8O_{16}$ and ClO_4 complexes based on the refined structural parameters are given in Fig. 3b.

If it is assumed that the intermolecular interactions are very similar in the three halide solutions with $n_{HO}=2$, differences between the experimental radial distribution curves will

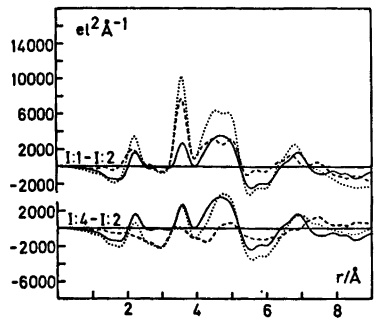

Fig. 7. Difference curves between the experimental radial distribution functions $D(r)-4\pi r^2\varrho_0$ for the halide solutions with $n_{HO}=2$ (dashed). The full-drawn curve is always subtracted from the dotted curve.

mainly reflect differences in the intramolecular interactions within the $M_4O_8O_{16}X_6$ complexes. Such difference curves obtained by subtracting the $D(r)-4\pi r^2\varrho_0$ function for solution I:2 from those of the other two halide solutions with $n_{HO}=2$ are shown in Fig. 7.

The difference curve for the chloride solutions has peaks in regions where the interactions involving the metal atoms are expected to occur according to the suggested structural model: 2.2 Å (M–O), 3.55 Å (M–M), 4–5 Å (M–O, M–Cl, M–M), and 6.2–7 Å (M–O, M–Cl) (compare Fig. 5) reflecting the higher scattering power of Hf compared to Zr.

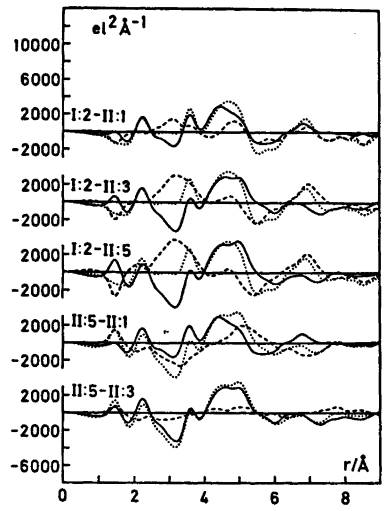

Fig. 8. Difference curves between the experimental radial distribution functions $D(r)-4\pi r^2\varrho_0$ for solution I:2 and three of the perchlorate solutions (dashed) and for the perchlorate solutions (dashed).

The difference curve for the zirconium halide solutions has peaks in regions where the interactions involving the halide ions are expected to occur according to the suggested structural model: 3.4 Å (X–O), 4.5–5.2 Å (Zr–X, X–O, X–X), and 7–7.7 Å (Zr–X, X–O, X–X) reflecting the difference in scattering power between Br and Cl.

Difference curves calculated by subtracting the $D(r)-4\pi r^2\varrho_0$ functions for the perchlorate solutions from that of solution I:2 (Fig. 8) show as main features (apart from the negative perchlorate peaks) peaks around 3.2 Å (Cl–O), 4.75 Å (Zr–Cl), and 7 Å (Zr–Cl) which strongly support the suggested structural models.

Difference curves calculated by subtracting the $D(r)-4\pi r^2\varrho_0$ functions for the solutions II:1 to II:4 from that of solution II:5 (Fig. 8) show a broad peak at about 5 Å. This increases in size as the difference in the perchlorate concentration increases.

The halide solutions with $n_{HO}=3$

On comparing the scattering curves in Fig. 1a it is obvious that the two halide solutions with $n_{HO}=3$ behave quite differently from those with $n_{HO}=2$. A structural change has occurred when the degree of hydrolysis has been increased. It is also seen from the scattering curves that the more hydrolyzed solutions seem to contain very large molecules. The Fourier inversions of the reduced intensity values (Figs. 2a and 3a) also have peaks at r values greater than 9 Å.

From a comparison between the $D(r)-4\pi r^2\varrho_0$ curves for the two structurally different types of halide solutions (Fig. 9), the following characteristics of the structure of the large molecules may be deduced: (1) The first coordination sphere of O atoms around Zr is not changed. It still contains eight O atoms at the same Zr–O distances as in the complex $[Zr_4(OH)_8(H_2O)_{16}]^{8+}$. (2) The peak at 3.6 Å (for $n_{HO}=2$) is higher and broader for the more hydrolyzed solutions. This means that in the large aggregates the number of Zr–Zr distances per Zr atom at 3.6 Å is larger than one. The peak sizes give

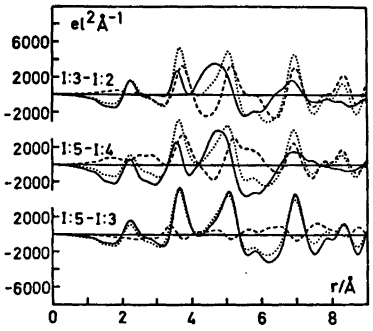

Fig. 9. Difference curves between the experimental radial distribution functions $D(r) - 4\pi r^2\varrho_0$ for the zirconium halide solutions (dashed).

about two such distances per Zr atom. The broadness of the peaks indicates a distribution of Zr – Zr distances in the region 3.55 – 3.75 Å. (3) The third peak in the $D(r) - 4\pi r^2\varrho_0$ curves has moved to higher r values as the degree of hydrolysis has been increased. Subtraction of the curve for the zirconium bromide (chloride) solution with $n_{HO} = 2$ from that of the corresponding solution with $n_{HO} = 3$ (Fig. 9) results in difference curves with a residual peak at about 5.15 Å (*i.e.* 3.65 $\sqrt{2}$ Å). Thus, if it is assumed that the second coordination sphere of O atoms about Zr is essentially the same, further hydrolysis of the tetramers gives large aggregates having more than 0.5 Zr – Zr distances per Zr atom in the region 5 – 5.15 Å. The peak sizes give about two such distances per Zr atom. (4) There is also a large peak at 6.95 Å which most probably is due mainly to Zr – Zr interactions. The size of the peak indicates about two Zr – Zr distances per Zr atom at a distance which is somewhat less than twice the mean shortest Zr – Zr distance in the large molecules (2×3.65 Å = 7.3 Å). (5) There is no clear indication of a coordination of halide ions in the second coordination sphere around Zr. This is seen from the featureless difference curve between the $D(r) - 4\pi r^2\varrho_0$ functions for the two halide solutions with $n_{HO} = 3$ in Fig. 9.

The scattering curves for the two zirconium halide solutions with $n_{HO} = 3$ are not similar to any of the diffraction patterns reported in the ASTM card index of the various modifications of ZrO_2 (cubic, tetragonal, or monoclinic).

Clearfield [21] has discussed a probable mechanism for the hydrolytic polymerization of the species $[Zr_4(OH)_8(H_2O)_{16}]^{8+}$. The polymerization is suggested to occur by the formation of double HO bridges between tetramers, the new bridges being at right angles to those already present. The arrangement is supposed to be irregular when just adding HO^- to a solution containing tetrameric Zr(IV) complexes, but it is supposed to be ordered after refluxing the Zr(IV) solution.

The scattering curves for the two zirconium halide solutions with $n_{HO} = 3$ may be explained by assuming randomly formed polymers according to Clearfield. The polymer drawn in Fig. 10 is one example of a complex containing about two Zr – Zr distances per Zr atom in each of the r regions around 3.65, 5.15, and 6.95 Å. It has, as a mean, $n_{HO} = 3$.

DISCUSSION

Radial distribution curves give only one-dimensional representations of the structures of the three-dimensional complexes in a solution. Many structural models that give a good explanation of the experimental data may therefore be derived. But from the scattering curves obtained here it seems reasonable to assume that the complex $M_4O_8O_{16}$ with a structure known from the solid state [9] is predominating in all the solutions investigated, halide as well as perchlorate solutions. The halide solutions with $n_{HO} = 3$ are, of course, excepted. The intensity data are, however, not very sensitive to changes in the parameters of interactions including only light atoms. Thus, a small rearrangement of the coordinated water

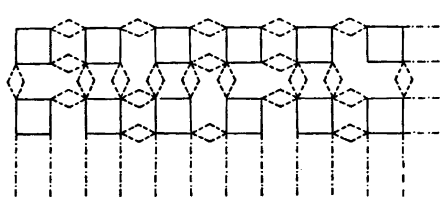

Fig. 10. A two-dimensional representation of a randomly formed polymer $[Zr_4(OH)_{12}(H_2O)_8]_n^{4+}$ The solid lined squares denote the original tetramers and the dashed lines represent new Zr – OH bonds formed by hydrolysis.

molecules in $M_4O_8O_{16}$ may not change the calculated curves significantly.

It seems unlikely that the halide ions which are not directly coordinated to the metal atom in the solid (Fig. 4) should enter the first coordination sphere in solution. In the crystal structure of, *e.g.*, $Zr(CH_3COCHCOCH_3)_3Cl$, where Zr(IV) is seven-coordinated, the Zr–Cl bond length is 2.47 Å.[22] The radial distribution curves (Figs. 2a and 3a) do not show any peaks in this region.

In the solid state two crystallographically different sites are occupied by the halide ions. They are called I and II in Fig. 4. With four halide ions statistically distributed over the eight II positions, the calculated difference curves in Figs. 2a and 3a show no pronounced peaks related to intramolecular interactions not included in the structural model for the zirconium halide solutions. For the hafnium chloride solution, however, there remains an unexplained peak at 4.3 Å which is too large to be related to highly damped intermolecular interactions only. This peak may be due to Hf–Cl and (or) Hf–O interactions within the second coordination sphere. Another explanation is that condensation into higher complexes has taken place. But there seems to be no reason to assume that complexes of higher nuclearity should occur in hafnium chloride than in zirconium halide solutions of the same degree of hydrolysis. Furthermore, when condensation occurs, the ultracentrifugation measurements indicate a higher average nuclearity for Zr.[23]

It might be possible to get a still better agreement between experimental and calculated scattering data by trying more complicated structural models for the halide solutions ($n_{HO}=2$) not necessarily based on or related to the halide positions I and II in the solid state. But the model including the II positions fractionally occupied seems to be the simplest one which adequately explains the scattering data. The contact distances to neighbouring O atoms are then 3.1–3.5 Å for the Cl^- and 3.2–3.6 Å for the Br^- ion. These values are roughly in agreement with the sum of the ionic radii.

Muha [10] in his early investigation of the structure of aqueous solutions of $MOX_2 \cdot 8H_2O$ (M=Zr or Hf, X=Cl or Br) explained his scattering data by assuming the existence of a complex $[M_4(OH)_8(H_2O)_{16}]X_8$. The structural parameters for the complex $M_4O_8O_{16}$ were taken from the old crystal structure determination by Clearfield and Vaughan.[8] Nevertheless Muha found residual peaks of about equal size at 4.6 and 7.3 Å for a 2 molal hafnium bromide solution. These peaks were attributed to Hf–Br interactions. Several structural models were tested, but the one based on halide ions in positions II were found to give the best agreement between experimental and calculated data for the hafnium halide solutions. The data did not permit a definite conclusion concerning the average number of chloride ions associated with a $Hf_4O_8O_{16}$ complex to be drawn, but for the bromide solutions the halide sites seemed to be fractionally occupied.

For the perchlorate solutions the difference curves in Fig. 3b are all very similar regardless of the degree of acidity. Thus it seems that the complex $Zr_4O_8O_{16}$ is formed rapidly when $HClO_4$ is added to hydrous ZrO_2 giving $ClO_4/Zr=2$, but that it remains intact on further acidification even after "equilibrating" the solutions for one month on the water bath. All the difference curves show broad peaks at about 2.9, 4.3, 5.25, 6.5, and 7.8 Å. The peak at 5.25 Å gets larger as the ClO_4/Zr ratio is increased. If the ClO_4 group enters the second coordination sphere around Zr the expected Zr–Cl distance would be about 5.25 Å. No quantitative analyses of the residual peaks were made due to the large number of ways for arranging ClO_4 about a $Zr_4O_8O_{16}$ complex.

The peak at 4.3 Å found in the difference curves of the hafnium chloride solution is seen also for the zirconium halide solutions, although of much smaller size. Thus, as a pronounced peak at this r value was found for the perchlorate solutions as well, it seems more likely that this peak is due mainly to M–O interactions from a second coordination sphere of water molecules rather than to interactions involving halide ions. Furthermore, the size of the peak is about the same for the zirconium bromide and chloride solutions.

For the most hydrolyzed perchlorate solution $n_{HO}=2.3$. Although $n_{HO}>2$ there seems to be no tendency towards formation of polymers, *e.g.*, of the type suggested in Fig. 10. The difference curve for solution II:1 in Fig. 3b has

no unexplained peaks around 3.65, 5.15, and 6.95 Å. Instead, it is similar to the difference curves for the perchlorate solutions with lower degrees of hydrolysis (II:2 – II:5).

A possible scheme for the formation of polymers with a random structure in the zirconium halide solutions with $n_{HO} = 3$ is:

$$4n\mathrm{Zr(OH)_4} + nx\mathrm{H_2O} + 4ny\mathrm{H_3O^+} \rightleftharpoons$$
$$[\mathrm{Zr_4O_x(OH)_{16-2x-4y}\ (H_2O)_{2x+8y}}]_n^{4y+}\ (y=1)$$

The factor x takes into account the possible formation of an O bridge and a coordinated water molecule instead of a double HO bridge in and (or) between some tetramers. The coordination number of Zr is assumed to be eight.

Acknowledgements. I wish to thank Dr. Georg Johansson for his interest in this work, Civ. ing. Magnus Sandström for valuable help in handling the computer programs, and B. Sc. Ian Duncan for revising the English of the text.

The work has been financially supported by the Swedish Natural Science Research Council. Computer time has been made available by the Computer Division of the National Swedish Office for Administrative Rationalization and Economy.

REFERENCES

1. Solovkin, A. S. and Tsvetkova, S. V. *Russ. Chem. Rev. 31* (1962) 655.
2. Caletka, R. *Chem. Listy 58* (1964) 349.
3. Hala, J. *U. S. At. Energy Comm., Accession No. 35508 Rept. No. UJV – 1066/64.*
4. Larsen, E. M. *Adv. Inorg. Chem. Radiochem. 13* (1970) 1, and references therein.
5. Hardy, C. J., Field, B. O. and Scargill, D. *J. Inorg. Nucl. Chem. 28* (1966) 2408.
6. Baglin, F. G. and Breger, D. *Inorg. Nucl. Chem. Lett. 12* (1976) 173.
7. Sillén, L. G. and Martell, A. (compilers) *Stability Constants of Metal-Ion Complexes*, Chem. Soc. Spec. Publ. No. 17 (1964); Suppl. No. 1, Spec. Publ. No. 25 (1971).
8. Clearfield, A. and Vaughan, P. A. *Acta Crystallogr. 9* (1956) 555.
9. Mak, T. C. W. *Can. J. Chem. 46* (1968) 3491.
10. Muha, G. M. and Vaughan, P. A. *J. Chem. Phys. 33* (1960) 194; Muha, G. M. *Univ. Microfilms L. C. Card No. Mic 60 – 1445, Diss. Abstr. 20* (1960) 4292.
11. Johansson, G. *Acta Chem. Scand. 20* (1966) 553.
12. Gaizer, F. and Johansson, G. *Acta Chem. Scand. 22* (1968) 3013.
13. Johansson, G. *Acta Chem. Scand. 25* (1971) 2787.
14. Johansson, G. and Sandström, M. *Chem. Scr. 4* (1973) 195.
15. Pocev, S. and Johansson, G. *Acta Chem. Scand. 27* (1973) 2146.
16. Cromer, D. T. and Waber, J. T. *Acta Crystallogr. 18* (1965) 104.
17. Stewart, R. F., Davidson, E. K. and Simpson, W. T. *J. Chem. Phys. 42* (1965) 3175.
18. Cromer, D. T. *Acta Crystallogr. 18* (1965) 17.
19. Cromer, D. T. *J. Chem. Phys. 50* (1969) 4857.
20. Compton, A. H. and Allison, S. K. *X-Rays in Theory and Experiment*, van Nostrand, New York 1935.
21. Clearfield, A. *Rev. Pure Appl. Chem. 14* (1964) 91.
22. von Dreele, R. B., Stezowski, J. J. and Fay, R. C. *J. Am. Chem. Soc. 93* (1971) 2887.
23. a. Johnson, J. S., Kraus, K. A. and Holmberg, R. W. *J. Am. Chem. Soc. 78* (1956) 26; b. Johnson, J. S. and Kraus, K. A. *Ibid.* 3937.

Received August 11, 1976.